

Controlled Assembly for Well-Defined 3D Bioarchitecture Using Two Active Enzymes

Dong Chung Kim,^{†,*,#,¶} Jung Inn Sohn,[§] Dejian Zhou,[‡] Thomas A. J. Duke,^{*,#} and Dae Joon Kang^{†,*}

[†]BK21 Physics Research Division, Department of Energy Science, Institute of Basic Science, SKKU Advanced Institute of Nanotechnology, Center for Nanotubes and Nanostructured Composites, Sungkyunkwan University, Suwon, 440-746, South Korea, [‡]Biological and Soft Systems, Cavendish Laboratory, University of Cambridge, 19 J J Thomson Avenue, Cambridge CB3 0HE, U.K., [§]Nanoscience Centre, University of Cambridge, 11 J J Thomson Avenue, Cambridge CB3 0FF, U.K., [‡]School of Chemistry and Astbury Centre for Structural Molecular Biology, University of Leeds, Woodhouse Lane, Leeds LS2 9JT, U.K., and [¶]Department of Human Nutrition and Food Science, Chungwoon University, Hongseong 350-701, South Korea. [#]Present address: London Centre for Nanotechnology, University College London, 17-19 Gordon Street, London WC1H 0AH, U.K.

ABSTRACT This paper reports that a bioarchitecture with two different active enzymes can be fabricated conveniently on a prepatterned surface by highly selective surface-templated layer-by-layer (LBL) assembly by coupling a bilayer of avidin/biotin-lactate oxidase (biotin-LOD) with a bilayer of avidin/biotin-horseradish peroxidase (biotin-HRP). The two different active enzymes can be utilized as excellent building blocks for the fabrication of well-defined 3D nanostructures with precise control of the position and height on the surface. In addition, the LBL assembled bienzyme structures are highly functional, and bioarchitectures based on LOD and HRP-mediated coupling reaction can be employed in a number of viable biosensing applications.

KEYWORDS: bioarchitecture · well-defined 3D nanostructure · lactate oxidase · horseradish peroxidase · LBL assembly

Three-dimensional (3D) nanostructures are vital in the field of nanotechnology including sensors, photonics, optoelectronics, microfluidics, and fuel cells.^{1–3} 3D nanostructures have been fabricated by applying various kinds of lithographic techniques to molecular self-assembly such as layer-by-layer (LBL) assembly,^{4,5} which is driven by electrostatic interaction, covalent bonding and specific interaction to create multilayer structures using charged polymers, nanoparticles, and biomolecules.^{6,7} One of the key considerations in fabrication of 3D nanostructures is the positioning of individual units such as polymers, proteins, and nanoparticles with nanometer precision.⁸ LBL assembly is a convenient nanofabrication protocol used to produce well-defined 3D nanostructures with biomolecules,^{9,10} which are versatile building blocks with unique functionality for bottom-up nanofabrication.^{11,12} Specific interactions between host and guest molecules is a facile driving force for LBL assembly of biomolecules.^{13,14} The specific interaction

between avidin and biotinylated biomolecules has been used as an ideal LBL assembly route to three-dimensional (3D) architecture due to the specific and strong interaction ($K_d \approx 10^{-15}$ M) of avidin–biotin.¹⁵

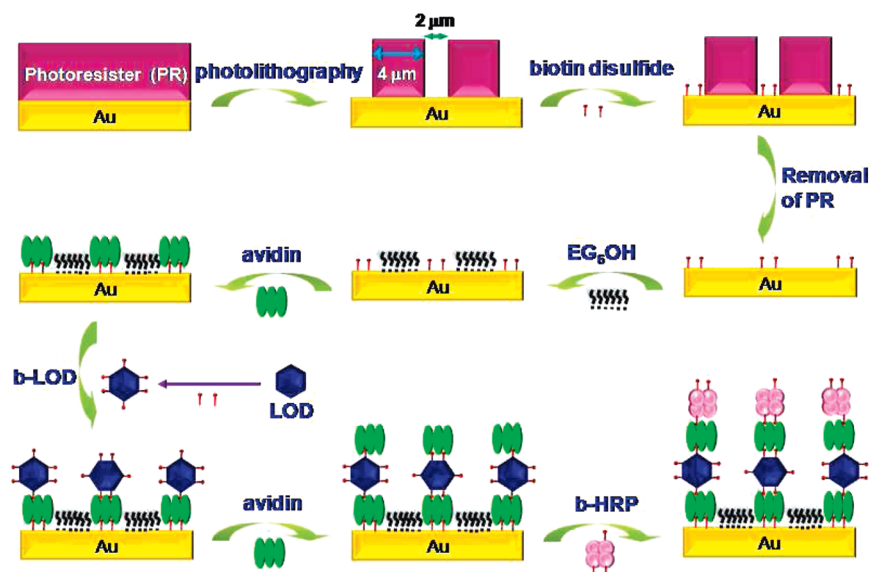
With fine control of the position, pattern size, and height, LBL assembly can be useful for fabricating novel surface bionanostructures. One approach to achieving the required precision is to use a patterned surface produced by photolithography¹⁶ or microcontact printing (μ CP)¹⁷ to guide LBL assembly on a surface. It was previously reported that well-defined multilayer enzyme structures could be achieved using a μ CP-patterned self-assembled monolayer (SAM) template to guide the LBL assembly of horseradish peroxidase (HRP).⁹ However, those previously reported techniques were limited to LBL-assembled functional bioarchitectures using only a *single* type of enzyme, that is, HRP.^{9,18} Recently bienzyme systems have been introduced for fabrication of biosensors.^{19,20} However, they are not applicable for fabrication of well-defined 3D nanostructures because control of height and position was not carried out. These studies did not provide any evidence, such as AFM or fluorescence data, for LBL assembly or the increase in height caused by the build-up of enzyme layers. For viable device applications, it is often more useful and convenient to integrate the enzymatic reactions onto a solid surface because positional control can be greatly facilitated. In particular, it is essential to control the placement of the fabricated structures on a sur-

*Address correspondence to djkkang@skku.edu.

Received for review June 10, 2009 and accepted February 4, 2010.

Published online February 24, 2010. 10.1021/nn900610u

© 2010 American Chemical Society



Scheme 1. Schematic diagram of the approach to manufacture a bio-architecture with two active enzymes *via* surface templated layer-by-layer assembly.

face in order to apply these bienzyme systems to possible photonic or optoelectronic devices.

This paper reports that a bioarchitecture with two different active enzymes can be conveniently fabricated on a prepatterned surface through highly selective surface-templated LBL assembly by coupling a bilayer of avidin/biotin-lactate oxidase (LOD) with a bilayer of avidin/biotin-HRP. The two different active enzymes can be utilized as excellent building blocks for the fabrication of well-defined 3D nanostructures with precise control of position and height on the surface. In addition, the LBL assembled bienzyme structures are highly functional, and bioarchitectures based on LOD and HRP-mediated coupling reaction can be employed in a number of viable biosensing applications. To the best of our knowledge, this is the first example of a functional bioarchitecture with precise control of the position and well-defined 3D nanostructures assembled from two different active enzymes on a patterned surface.

RESULTS AND DISCUSSION

Layer-by-Layer Assembly for Well-Defined 3D Bioarchitecture.

A gold surface was patterned on the micrometer scale with self-assembled monolayers (SAMs) of a biotin-terminated thiol and a hexa(ethylene glycol)-terminated thiol. The biotin-terminated SAM was used to anchor the avidin to the gold surface, while the hexa(ethylene glycol) terminated SAM was used to block the nonspecific adsorption of the proteins. It was reported that hexa(ethylene glycol)-terminated SAM is quite effective in resisting the nonspecific adsorption of biomolecules.^{9,11,21} The patterned surfaces were then used as a template for LBL assembly of the avidin and biotinylated enzymes. Biotin-horseradish peroxidase (biotin-HRP), each conjugated with an average of

2.3 biotins, and biotin-lactate oxidase (biotin-LOD), each conjugated with an average of 10.2 biotins, were used as two active enzymes to build the functional bioarchitecture with a well-defined 3D nanostructure. Avidin acts as a biocompatible linker between the biotin-LOD and the biotin-HRP due to the strong biotin–avidin interaction ($K_d \approx 10^{-15}$ M).¹⁰

Scheme 1 shows the approach to constructing a bienzyme-based bioarchitecture. The gold surface was first patterned by standard photolithography and the micrometer-sized bare gold regions were then functionalized with a biotin-terminated SAM. After stripping off the photoresist, 11-mercaptoundecylhexa (ethylene glycol) alcohol (EG₆OH) was added to fill the micrometer-sized gaps lacking the biotin terminated SAM. Avidin was then assembled specifically onto the biotinylated SAM regions by its two lower biotin-binding sites. This leaves the other two biotin-binding sites on the opposite side of the avidin available for biotin-LOD binding because avidin has an almost cubic shape with the two pairs of biotin-binding pockets arranged on the opposite sides of the molecule.^{22,23} The build-up of the biotin-LOD on the avidin layer produces a biotin terminated outmost layer, which is then used to construct a second avidin layer followed by a further biotin-HRP layer. This 3D bienzyme structure can be utilized as a lactate sensing device because the LOD and HRP are successively assembled into the LBL structures.

AFM Images of LBL-Assembled Bioarchitectures. The enzymes were assembled on micrometer scale patterns and the layer thickness was measured as a function of the LBL assembly using atomic force microscopy (tapping mode in air) to confirm that the LBL assembly of avidin/biotin-LOD/avidin/biotin-HRP can be well-controlled. The topographic evolution of the protein

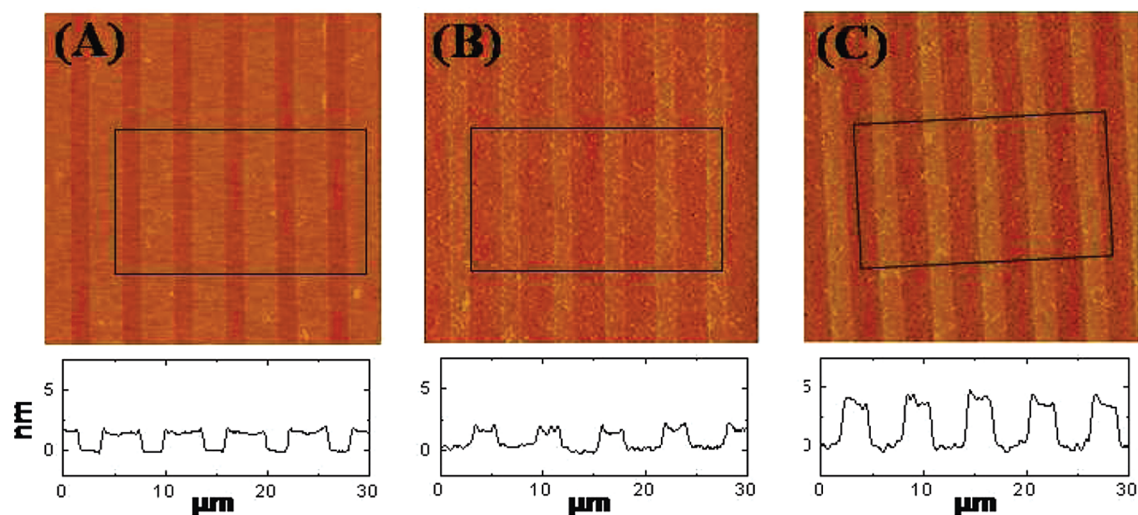


Figure 1. AFM topographic images of the 3D structures assembled from avidin/biotin-LOD and avidin/biotin-HRP. The corresponding average line scan profile is depicted beneath each image. (A) A μ -patterned template with 4 μm EG₆OH stripes separated by 2 μm biotin-thiol stripes on a flat thin-gold coated surface. The EG₆OH region is ~ 1.5 nm taller than the biotin-thiol region. (B) After assembling a bilayer of avidin/biotin-LOD, the protein stripes are ~ 1.7 nm higher than the EG₆OH stripes. (C) After assembling the avidin/biotin-LOD/avidin/biotin-HRP stripes, the height of the enzyme stripes is ~ 3.7 nm above the resistive background.

patterns after the LBL assembly process was also monitored. Figure 1A shows a topographic AFM image of a micropatterned SAM template with 2 μm SAM stripes of the biotin thiol separated by 4 μm SAM stripes of the EG₆OH on a flat surface thinly coated with gold. The EG₆OH stripes were ~ 1.5 nm taller than the biotin-thiol stripes. After a bilayer of avidin/biotin-LOD was assembled onto the biotin stripes, the topographic contrast between the protein and EG₆OH stripes was reversed (Figure 1B). The protein stripes were ~ 1.7 nm taller than the EG₆OH stripes, presumably because the proteins assembled selectively onto the biotin stripes. There is little evidence of nonspecific adsorption on the resist stripes. In addition, the nonspecifically adsorbed proteins on the resistive stripes could be removed by treating the surface with a surfactant (0.1% Tween in PBS). Multilayer structures with a protein layer configuration of avidin/biotin-LOD/avidin/biotin-HRP can be readily fabricated using a surfactant rinse between each assembly step. Figure 1C shows a topographic image of the patterned surface after the assembly of avidin/biotin-LOD/avidin/biotin-HRP. The height of the protein stripes was ~ 3.7 nm above the resistive background. The thicknesses of the avidin/biotin-LOD bilayer (~ 3.2 nm) and avidin/biotin-LOD/avidin/biotin-HRP quadruple layer (~ 5.2 nm) were smaller than the combined thickness of the closely packed protein layers using the molecular dimensions of HRP and avidin (*ca.* 8–10 nm).^{9,24} This is not unusual and similar results have been reported elsewhere.^{9–11,18,25} Since the samples for AFM measurements were rinsed with distilled water to remove salt and then dried by N₂ gas, the assembled proteins might have been partially unfolded and denatured, thus causing the decrease in height of protein layers.⁹ The AFM topographic images show that

the 3D enzyme structures are well-controlled on the functional pattern region through LBL assembly. In addition, the increase in height of the protein stripes after each assembly step is consistent with the fluorescence data (Figure 2) which was taken using fluorophore-labeled biotin-LOD and biotin-HRP.

Fluorescence Images of LBL-Assembled Bioarchitectures. Figure 2 shows a scanning confocal fluorescence image using fluorophore-labeled enzymes on the micropatterned surface. The biotin-LOD was labeled with the Cy3 dye in order to monitor the growth of the avidin/biotin-LOD-Cy3 assembly by measuring the emission at 585 nm with a scanning confocal fluorescence microscope. Cy5-labeled biotin-HRP was used to produce microscale stripes of an avidin/biotin-HRP-Cy5 assembly on top of the avidin/biotin-LOD-Cy3 stripes, leading to a change in the emission wavelength (from 585) to 650 nm. The fluorescence was exclusively detected almost from the protein stripes with very low background

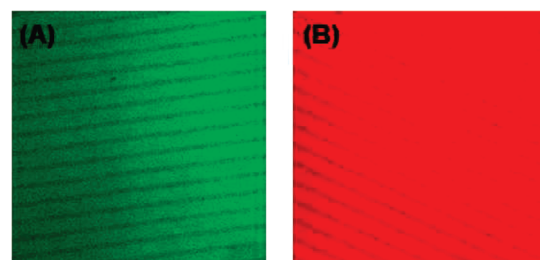


Figure 2. Fluorescence images of the LBL assembly of avidin/biotin-LOD and avidin/biotin-LOD/avidin/biotin-HRP. (A) Cy3-labeled biotin-LOD assembled on μ -patterned biotin/avidin stripes with EG₆OH gaps on a thin-gold-layer coated glass slide under laser excitation at 543 nm. (B) Cy5-labeled biotin-HRP assembled on μ -patterned biotin/avidin/biotin-LOD-Cy3/avidin stripes with EG₆OH gaps on a thin-gold-layer coated glass slide under laser excitation at 633 nm.

fluorescence, suggesting that the EG₆OH SAM is quite effective in preventing the nonspecific adsorption of proteins. The AFM topography and fluorescence images obtained from the green (Figure 2A) and red channels (Figure 2B) clearly demonstrate the regular and successively well-controlled LBL build-up of a multilayer enzyme structure with nanometer precision. This shows that the highly selective surface-templated LBL assembly is a facile yet powerful approach for assembling functional and well-defined 3D structures with two different fluorophore-labeled biomolecules, and can be applied to photonic or optoelectronic devices, such as organic-based LED.

Catalytic Activity of LBL-Assembled

Bioarchitectures. A colorimetric-based assay was used to determine the activity of the multilayer avidin/biotin-LOD/avidin/biotin-HRP structures rinsed with PBS only, without the surfactant. This bienzyme system converts the colorless enzymatic reaction of LOD into a strongly colored one, which is visible to the naked eye. In the presence of oxygen, LOD catalyzes the conversion of L-lactate into pyruvate and H₂O₂. The H₂O₂ is then used as an oxidant by the nearby HRP in the assembled bioarchitecture to convert the noncolored Amplex red into colored resorufin,²⁶ which absorbs strongly at 571 nm, as illustrated schematically in Figure 3A. It is also possible that a single type of LOD enzyme without HRP can be used for the detection of lactate. However, its detection performance is reported to be much worse compared with the bienzyme systems in combination with oxidase and HRP.^{19,20} The bienzyme system can have two geometries (monolayer and bilayer). The first monolayer geometry is realized by the immobilization of both LOD and HRP in the same layer on a surface. The second geometry is composed of an enzyme bilayer where the inner layer is composed of LOD and HRP is located on LOD layer by LBL assembly. The amount of immobilized enzymes in the bilayer enzyme geometry is two times higher than that in the monolayer enzyme geometry. Therefore the bilayer system is better suited to biosensing applications. Furthermore the bienzyme system of LOD and HRP is essential for colorimetric measurement of lactate. The changes in absorbance at different time intervals for the bienzyme system were measured, and the results are shown in Figure 3B. There was a linear increase in absorbance with increasing incubation time within a period of 30 min, suggesting that the bioarchitecture is catalytically active and maintains the same rate as a function of the incubation

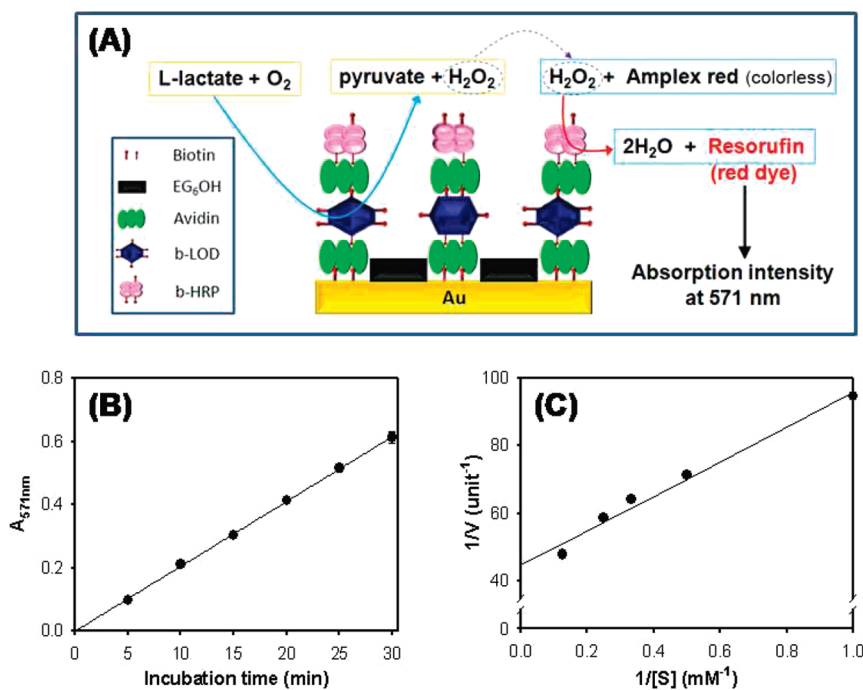


Figure 3. (A) Schematic diagram showing the reaction scheme for the two enzymatic reactions of the immobilized avidin/biotin-LOD/avidin/biotin-HRP assembly. (B) The catalytic activity of the bioarchitecture on a μ -patterned surface. Plot of the absorbance at 571 nm as a function of the incubation time. (C) The reaction rate of the bioarchitecture on μ -patterned surface as a function of the L-lactate concentration. Plot of the reaction rate as a function of the L-lactate concentration.

time. When the oxidative reaction of Amplex red in the same bioarchitecture without L-lactate under identical conditions was monitored as a control experiment, there was no change in the absorbance over the 30 min period (data not shown). This confirms that the observed color change is due to the coupled enzymatic reaction, and not to the auto-oxidation of Amplex red by the solution oxygen.

The assembly efficiency between avidin/biotin-HRP/avidin/biotin-LOD and avidin/biotin-LOD/avidin/biotin-HRP on gold surface was investigated. It was found that the LOD activity of avidin/biotin-HRP/avidin/biotin-LOD seemed to linearly increase with the reaction time while its magnitude remained quite low. Furthermore, no clear dependency of its reaction rate on L-lactate concentration was found (data not shown). When the HRP activity of avidin/biotin-HRP/avidin/biotin-LOD was measured in order to confirm this, its activity was only $\sim 25\%$ compared with that of avidin/biotin-HRP without avidin/biotin-LOD (data not shown). This is thought to be ascribed to steric hindrance.⁹ On the basis of this control experiment we conclude that the assembly of avidin/biotin-LOD/avidin/biotin-HRP is better-suited for the quantification of the L-lactate concentration.

The response of the avidin/biotin-LOD/avidin/biotin-HRP assembly in the presence of different concentrations of L-lactate was monitored to demonstrate the potential of such enzyme structures as an analytical kit for determining the L-lactate content based on the LOD

and HRP coupled reactions. The rate of the enzymatic reaction was found to be dependent on the L-lactate concentration (Figure 3C). The L-lactate content in a commercially available yogurt was also measured to demonstrate the practical applications of the system because the L-lactate content is considered to be an important index for determining the degree of fermentation in fermented products, such as kimchi, beer, and yogurt. The L-lactate content in a commercial liquid yogurt measured by our bioarchitecture was $0.48 \pm 0.02\%$ (w/w) which is within the acceptable commercial range.^{27,28} This demonstrates that our bienzyme-based bioarchitecture is well-suited for determining the L-lactate content in fermented products. The stability of the bioarchitecture of avidin/biotin-LOD/avidin/biotin-HRP was investigated. The bioarchitecture was stored in 50 mM sodium phosphate buffer (pH 7.2) solution at 4 °C. The activity gradually decreased with storage time and was observed to be ~60% of its initial activity after 10 days storage (data not shown). This result is in good agreement with the results reported elsewhere.^{29,30} HRP was reported to be reversibly and/or irreversibly inactivated at high concentration of hydrogen peroxide, an inactivating agent of HRP.^{29,30} The partial conformational change of 3D protein structures that slowly proceeded during the storage period in solution could facilitate the inactivation of HRP by hydrogen peroxide, and thus decrease the activity of bioarchitecture.

This LBL-assembled bienzyme system can be exploited to fabricate an electrochemical biosensor

on other functional nanomaterials such as nanoparticles and carbon nanotubes. The nanomaterials can be a potential platform in LBL assembly of biomolecules for the fabrication of electrochemical sensors due to their high surface area and high surface free energy.³¹ For example, the use of carbon nanotube in LBL assembly of enzymes was extremely suitable for electrochemical sensing due to its high surface-to-volume ratio, its biocompatibility, and the fast electron-transfer mediation for wide range of electroactive species.^{32,33}

In conclusion, a functional bioarchitecture with precise control of the position and well-defined 3D nanostructures was successfully fabricated using a micropatterned SAM template to guide the LBL assembly of avidin/biotin-LOD and avidin/biotin-HRP. AFM and fluorescence data demonstrated that this method precisely controls the position and height of the bienzyme structures on the micropatterned surface with nanometer precision. The assembled bioarchitecture possesses the catalytic activities of both LOD and HRP. The enzyme reaction rate of the bioarchitecture was dependent on the L-lactate concentration. In principle the enzyme architectures can be miniaturized easily to the nanoscale using a nanoscale surface template, which will provide an opportunity to assemble active 3D enzyme nanostructures. The use of multiple enzyme constituents combined with well-controlled LBL assembly may lead to the development of highly miniaturized biosensors, biocatalysts, and biochips with enhanced functionality.

METHODS

Materials. Biotin disulfide *N*-hydroxysuccinimide ester (biotin disulfide), lactate oxidase, L-lactate, phosphate buffered saline (PBS), and avidin were purchased from Sigma-Aldrich (Dorset, U.K.). Biotin conjugated horseradish peroxidase (biotin-HRP) and Amplex red were obtained from Invitrogen (Paisley, U.K.). The EZ-link sulfo-NHS-SS biotinylation kit and 1-ethyl-3-(3-dimethylaminopropyl) carbodiimide hydrochloride (EDC) were supplied by Pierce Biotechnology (Rockford, IL). Cy3 hydrazide and Cy5 hydrazide were obtained from GE Healthcare (Bucks, U.K.). 11-Mercaptoundecylhexa (ethylene glycol) alcohol (EG₆OH) was synthesized and purified as described elsewhere.¹¹ PBS solution (10 mM phosphate, 150 mM NaCl, and pH 7.4) was prepared using ultrapure UHQ water (resistance > 18 MΩ · cm), and then filtered with a syringe filter (0.2 μm pore size, Whatman plc., Middlesex, U.K.) prior to use. The solutions of avidin, biotin-LOD, and biotin-HRP were prepared in PBS. Biotin-disulfide was dissolved in *N,N*-dimethylformamide and then diluted with UHQ water to make a 1 mM solution.

Preparation of Biotinylated Lactate Oxidase. Biotin was conjugated to lactate oxidase (LOD) using a published procedure.³⁴ A 500 μL portion of a solution of 1 mg/mL lactate oxidase from *Peidococcus* sp. (>20 units/mg) in PBS was mixed with 100 μL of 2 mg/mL sulfo-NHS-SS-biotin in PBS and incubated at room temperature for 2 h. The reaction mixture was applied to a desalt spin column (Pierce Biotechnology) equilibrated with PBS. The column was placed into a 15 mL collection tube and centrifuged using a Harrier 18/80 refrigerated centrifuge (Sanyo Scientific, Itasca, Ill, USA) at 1000g for 2 min. The collected flow-through solution was the purified biotin-LOD conjugate sample. The biotin

content in biotin-LOD was determined by competitive replacement of 2-(4-hydroxyphenylazo) benzoic acid bound to avidin.

Micropatterning by Photolithography and LBL Assembly. Silicon substrates coated with a thin layer of gold (8 nm thick gold layer with 2 nm Cr adhesion layer and roughness <0.5 nm) were prepared by thermal evaporation (deposition rate = 0.01 nm/sec). A micropattern with 2 μm stripes separated by 4 μm gaps was fabricated using a standard photolithography procedure.^{35,36} After photolithography, the micropatterned photoresist on the gold substrate was incubated with a 1 mM solution of biotin-disulfide in UHQ water for 1.5 h in order to fill the bare gold regions with a biotin-terminated SAM. The substrate was rinsed with UHQ water to remove the unbound biotin-disulfide. The photoresist was then stripped off the substrate in an acetone bath for 20 min, rinsed with UHQ water, and then dried with a N₂ gas blow. The exposed regions were filled with a SAM of EG₆OH by dipping the substrate in a 2 mM solution of EG₆OH in methanol for 1.0 h, rinsing with methanol, and then drying with N₂. The gold substrate with 2 μm biotin stripes separated by 4 μm EG₆OH resist regions was soaked in PBS for 10 min before being used as a template for LBL assembly. The substrate was incubated with a 0.1 mg/mL avidin solution for 0.5 h, rinsed with PBS, and soaked in a 0.2 mg/mL biotin-LOD solution for 0.5 h followed by washing with PBS. This produced an avidin/biotin-LOD bilayer. The bienzyme multilayer structure was assembled in a similar manner using avidin (0.1 mg/mL) and biotin-HRP (0.2 mg/mL).

Atomic Force Microscopy. The micropatterned SAM stripes on the gold substrate were analyzed by atomic force microscopy (AFM). The regions of biotin terminated SAM, avidin/biotin-LOD,

and avidin/biotin-LOD/avidin/biotin-HRP were compared with the EG₆OH resist regions. Each sample was treated individually with a surfactant (0.1% Tween 20 in PBS) for 1.5 h, rinsed with UHQ water and dried with N₂ gas before the AFM measurements. All AFM measurements were carried out using a Digital Instrument (Santa Barbara, CA, USA) Dimension 3100 AFM with a Nanoscope IV controller at 24 ± 1 °C.^{9,37,38} Ultrasharp MikroMasch (Willsonville, OR) silicon cantilevers (NSC15/Al BS, 125 μm long, tip radius <10 nm, spring constant ~40 N/m, and resonant frequency ~325 kHz) were used. The images were collected at a scan rate of 0.5–1.0 Hz with 512 × 512 pixels per image and analyzed using Nanoscope image analyzing software (version 6.12) with first-order flattening. Topographic images were taken under light tapping to minimize the effect of tip compression on the bioassembly features.

Fluorescence Imaging. Cy5-labeled biotin-HRP (biotin-HRP-Cy5) and Cy3-labeled biotin-LOD (biotin-LOD-Cy3) were prepared from the EDC-mediated coupling reaction.³⁹ A 1 mL portion of 1 mg/mL biotin-HRP was mixed with 100 μL of 5 mg/mL Cy5 hydrazide and 100 μL of 10 mg/mL EDC in PBS and incubated for 15 h at ambient temperature in the dark. The product was centrifuged at 10000g for 5 min. The supernatant was loaded onto a 10 mL gel filtration column that had been equilibrated with PBS, and biotin-HRP-Cy5 was then eluted with PBS. Biotin-LOD-Cy3 was prepared in a similar manner using biotin-LOD and Cy3 hydrazide solutions. The Cy3 labeled product was purified on a gel filtration column. LBL assembly of biotin-LOD-Cy3 and biotin-HRP-Cy5 was carried out under the same conditions described above. The gold substrate (3 nm thick gold layer with a 0.5 nm Cr adhesion layer on a glass slide) with the 10 μm biotin stripes separated by 5 μm EG₆OH gaps was used as a template for LBL assembly. The substrates with avidin/biotin-LOD-Cy3 and avidin/biotin-LOD-Cy3/avidin/ biotin-HRP-Cy5 were prepared independently for the fluorescence measurements. Each sample was treated with a surfactant (0.1% Tween 20 in PBS) for 1.5 h, rinsed with water, and dried before the fluorescence measurements. The samples were analyzed by confocal microscopy using a Zeiss LSM 510 laser scanning confocal microscope with a 40× objective.^{40,41} The images were collected using excitation lasers of 543 nm for Cy3 and 633 nm for Cy5 with conventional Cy3 and Cy5 filter sets.

Measurement of the Catalytic Activity in the LBL Assembly. The bioarchitectures assembled on the patterned gold substrates (1 × 1 cm²) containing 10 μm biotin stripes separated by 5 μm EG₆OH gaps were used to measure the immobilized LOD activity. The LOD activity was measured in PBS containing 10 mM L-lactate and 50 μM Amplex red in a quartz cuvette (1 cm path length) with total volume of 3 mL. The enzyme activity was examined by monitoring the peak absorption of resorufin at 571 nm at different time intervals on a Cary 300 Bio UV–visible spectrophotometer (Varian Ltd., Oxford, UK) at 24 ± 1 °C for 30 min. One unit of LOD activity was defined as the change in absorbance at 571 nm of 1 A unit per minute (1 unit = 1 A₅₇₁/min). The LBL assembly was used to determine the L-lactate content. L-Lactate was dissolved in PBS to a lactate concentration of 1–8 mM. The bioarchitecture was incubated in PBS containing various L-lactate concentrations and 100 μM Amplex red in a quartz cuvette with a total volume of 3 mL for 5 min. 1/[S] versus 1/V was plotted, where [S] and V are the L-lactate concentration and initial reaction rate, respectively. The L-lactate content in a commercial liquid yogurt was also measured using the bioarchitecture.

Acknowledgment. This work was supported by grants NRF-20090094026 (Priority Research Centers Program), 2009-00591 (KICOS Global Partnership Program) and R31-2008-000-10029-0 (World Class University Program).

REFERENCES AND NOTES

- Shir, D. J.; Jeon, S.; Liao, H.; Highland, M.; Cahill, D. G.; Su, M. F.; El-Kady, I. F.; Christodoulou, C. G.; Bogart, G. R.; Hamza, A. V. *et al.* Three-Dimensional Nanofabrication with Elastomeric Phase Masks. *J. Phys. Chem. B* **2007**, *111*, 12945–12958.
- Shir, D. J.; Nelson, E. C.; Chen, Y. C.; Brzezinski, A.; Liao, H.; Braun, P. V.; Wiltzius, P.; Bogart, K. H. A.; Rogers, J. A. Three-Dimensional Silicon Photonic Crystals Fabricated by Two Photon Phase Mask Lithography. *Appl. Phys. Lett.* **2009**, *94*, 011101.
- Jeon, S.; Park, J. -U.; Cirelli, R.; Yang, S.; Heitzman, C. E.; Braun, P. V.; Kenis, P. J. A.; Rogers, J. A. Fabricating Complex Three-Dimensional Nanostructures with High-Resolution Conformable Phase Masks. *Proc. Natl. Acad. Sci. U.S.A.* **2004**, *101*, 12428–12433.
- Miyake, T.; Tani, T.; Kato, K.; Zako, T.; Funatsu, T.; Ohdomari, I. Selective Improvement in Protein Nanopatterning with a Hydroxyl-Terminated Self-Assembled Monolayer Template. *Nanotechnology* **2007**, *18*, 305304.
- Mendes, P. M.; Yeung, C. L.; Preece, J. A. Bio-Nanopatterning of Surfaces. *Nanoscale Res. Lett.* **2007**, *2*, 373–384.
- Zhang, X.; Chen, H.; Zhang, H. Layer-By-Layer Assembly: From Conventional to Unconventional Methods. *Chem. Commun.* **2007**, 1395–1405.
- Ariga, K.; Hill, J. P.; Ji, Q. Layer-By-Layer Assembly as a Versatile Bottom-Up Nanofabrication Technique for Exploratory Research and Realistic Application. *Phys. Chem. Chem. Phys.* **2007**, *9*, 2319–2340.
- Crespo-Biel, O.; Ravoo, B. J.; Reinhoudt, D. N.; Huskens, J. Noncovalent Nanoarchitectures on Surfaces: From 2D to 3D Nanostructures. *J. Mater. Chem.* **2006**, *16*, 3997–4021.
- Rauf, S.; Zhou, D.; Abell, C.; Klenerman, D.; Kang, D. J. Building Three-Dimensional Nanostructures with Active Enzymes by Surface Templated Layer-By-Layer Assembly. *Chem. Commun.* **2006**, 1721–1723.
- Beissenhirtz, M. K.; Scheller, F. W.; Lisdat, F. A Superoxide Sensor Based on a Multilayer Cytochrome C Electrode. *Anal. Chem.* **2004**, *76*, 4665–4671.
- Zhou, D.; Bruckbauer, A.; Ying, L.; Abell, C.; Klenerman, D. Building Three-Dimensional Surface Biological Assemblies at the Nanometer Scale. *Nano. Lett.* **2003**, *3*, 1517–1520.
- Whitesides, G. M.; Ostuni, E.; Takayama, S.; Jiang, X.; Ingber, D. E. Soft Lithography in Biology and Biochemistry. *Annu. Rev. Biomed. Eng.* **2001**, *3*, 335–373.
- Kong, D. Y.; Wang, Z. L.; Lin, C. K.; Quan, Z. W.; Li, Y. Y.; Li, C. X.; Lin, J. Biofunctionalization of CeF₃Tb³⁺ Nanoparticles. *Nanotechnology* **2007**, *18*, 075601.
- Jung, Y.; Lee, J. M.; Jung, H.; Chung, B. H. Self-Directed and Self-Oriented Immobilization of Antibody by Protein G-DNA Conjugate. *Anal. Chem.* **2007**, *79*, 6534–6541.
- Padeste, C.; Steiger, B.; Grubelnik, A.; Tiefenauer, L. Molecular Assembly of Redox-Conductive Ferrocene–Streptavidin Conjugates towards Bioelectrochemical Devices. *Biosens. Bioelectron.* **2004**, *20*, 545–552.
- Mooney, J. F.; Hunt, A. J.; McIntosh, J. R.; Liberko, C. A.; Walba, D. M.; Rogers, C. T. Patterning of Functional Antibodies and Other Proteins by Photolithography of Silane Monolayers. *Proc. Natl. Acad. Sci. U.S.A.* **1996**, *93*, 12287–12291.
- Michel, R.; Reviakine, I.; Sutherland, D.; Fokas, C.; Csucs, G.; Danuser, G.; Spencer, N. D.; Textor, M. A Novel Approach to Produce Biologically Relevant Chemical Patterns at the Nanometer Scale: Selective Molecular Assembly Patterning Combined with Colloidal Lithography. *Langmuir* **2002**, *18*, 8580–8586.
- Limoges, B.; Savéant, J. -M.; Yazidi, D. Quantitative Analysis of Catalysis and Inhibition at Horseradish Peroxidase Monolayers Immobilized on an Electrode Surface. *J. Am. Chem. Soc.* **2003**, *125*, 9192–9203.
- Delvaux, M.; Walcarius, A.; Demoustier-Champagne, S. Bifunctional HRP-GOx-modified Gold Nanoelectrodes for the Sensitive Amperometric Detection of Glucose at Low Overpotentials. *Biosens. Bioelectron.* **2005**, *20*, 1587–1594.
- Wang, J.; Liu, G.; Lin, Y. Amperometric Choline Biosensor Fabricated through Electrostatic Assembling of Bifunctional Polyelectrolyte Hybrid Layers on Carbon Nanotubes. *Analyst* **2006**, *131*, 477–483.

21. Lasseeter, T. L.; Clare, B. H.; Abbott, N. L.; Hamers, R. J. Covalently Modified Silicon and Diamond Surfaces: Resistance to Nonspecific Protein Adsorption and Optimization for Biosensing. *J. Am. Chem. Soc.* **2004**, *126*, 10220–10221.
22. Pugliese, L.; Coda, A.; Malcovati, M.; Bolognesi, M. Three-Dimensional Structure of the Tetragonal Crystal Form of Egg-White Avidin in its Functional Complex with Biotin at 2.7 Å Resolution. *J. Mol. Biol.* **1993**, *231*, 698–710.
23. Anzai, J. I.; Kobayashi, Y.; Suzuki, Y.; Takeshita, H.; Chen, Q.; Osa, T.; Hoshi, T.; Du, X. Y. Enzyme Sensors Prepared by Layer-by-Layer Deposition of Enzymes on a Platinum Electrode through Avidin–Biotin Interaction. *Sens. Actuators B: Chem.* **1998**, *52*, 3–9.
24. Otsuka, I.; Yaoita, M.; Higano, M.; Nagashima, S.; Kataoka, R. Tapping Mode AFM Study on the Surface Dynamics of a Single Glucose Oxidase Molecule on a Au(111) Surface in Water with Implication for a Surface-Induced Unfolding Pathway. *Appl. Surf. Sci.* **2004**, *235*, 188–196.
25. Rao, S. V.; Anderson, K. W.; Bachas, L. G. Controlled Layer-by-Layer Immobilization of Horseradish Peroxidase. *Biotechnol. Bioeng.* **1999**, *65*, 389–396.
26. Hasebe, Y.; Gu, T.; Fueki, T. Lactate Biosensor Based on Coupled Lactate Oxidase/Peroxidase System Incorporated into the DNA/Poly(allylamine) Polyelectrolyte Membrane. *Sens. Lett.* **2005**, *3*, 304–308.
27. Olieman, C.; de Vries, E. S. Determination of D- and L-Lactic Acid in Fermented Dairy Products with HPLC. *Neth. Milk Dairy J.* **1988**, *42*, 111–120.
28. Tamine, A. Y.; Robison, R. K. *Yogurt-Science and Technology*; Pergamon Press: Oxford, 1985; p 300.
29. Towne, V.; Will, M.; Oswald, B.; Zhao, Q. Complexities in Horseradish Peroxidase-Catalyzed Oxidation of Dihydroxyphenoxazine Derivatives: Appropriate Ranges for pH Values and Hydrogen Peroxide Concentrations in Quantitative Analysis. *Anal. Biochem.* **2004**, *334*, 290–296.
30. Goodwin, D. C.; Grover, T. A.; Aust, S. D. Roles of Efficient Substrates in Enhancement of Peroxidase-Catalyzed Oxidations. *Biochemistry* **1997**, *36*, 139–147.
31. Yang, H.; Zhu, Y. A High Performance Glucose Biosensor Enhanced via Nanosized SiO₂. *Anal. Chim. Acta* **2005**, *554*, 92–97.
32. Balasubramanian, K.; Burghard, M. Biosensors Based on Carbon Nanotubes. *Anal. Bioanal. Chem.* **2006**, *385*, 452–468.
33. Patolsky, F.; Weizmann, Y.; Willner, I. Long-Range Electrical Contacting of Redox Enzymes by SWCNT Connectors. *Angew. Chem., Int. Ed.* **2004**, *43*, 2113–2117.
34. Hoshi, T.; Anzai, J.; Osa, T. Controlled Deposition of Glucose Oxidase on Platinum Electrode Based on an Avidin/Biotin System for the Regulation of Output Current of Glucose Sensors. *Anal. Chem.* **1995**, *67*, 770–774.
35. Lee, K. N.; Shin, D. S.; Lee, Y. S.; Kim, Y. K. Protein Patterning by Virtual Mask Photolithography Using a Micromirror Array. *J. Micromech. Microeng.* **2003**, *13*, 18–25.
36. Koep, E.; Compson, C.; Liu, M.; Zhou, Z. A Photolithographic Process for Investigation of Electrode Reaction Sites in Solid Oxide Fuel Cells. *Solid State Ionics* **2005**, *176*, 1–8.
37. Zhou, D.; Sinniah, K.; Abell, C.; Rayment, T. Label-Free Detection of DNA Hybridization at the Nanoscale: A Highly Sensitive and Selective Approach Using Atomic-Force Microscopy. *Angew. Chem., Int. Ed.* **2003**, *42*, 4934–4937.
38. Jandt, K. D. Atomic Force Microscopy of Biomaterials Surfaces and Interfaces. *Surf. Sci.* **2001**, *491*, 303–332.
39. DeSilva, N. S.; Ofek, I.; Crouch, E. C. Interactions of Surfactant Protein D with Fatty Acids. *Am. J. Respir. Cell Mol. Biol.* **2003**, *29*, 757–770.
40. Bruckbauer, A.; Zhou, D.; Kang, D. J.; Korchev, Y. E.; Abell, C.; Klenerman, D. An Addressable Antibody Nanoarray Produced on a Nanostructured Surface. *J. Am. Chem. Soc.* **2004**, *126*, 6508–6509.
41. Segers-Nolten, G. M. J.; Wyman, C.; Wijgers, N.; Vermeulen, W.; Lenferink, A. T. M.; Hoeijmakers, J. H. J.; Greve, J.; Otto, C. Scanning Confocal Fluorescence Microscopy for Single Molecule Analysis of Nucleotide Excision Repair Complexes. *Nucleic Acids Res.* **2002**, *30*, 4720–4727.